J. Biochem. **120**, 126-132 (1996)

^{1}H NMR Probes for Inter-Segmental Hydrogen Bonds in Myoglobins

Yasuhiko Yamamoto[1]

Department of Chemistry, University of Tsukuba, Tsukuba, Ibaraki 305

Received for publication, February 20, 1996

NMR signals arising from the HisB5 $N_\delta H$ and HisEF5 $N_\epsilon H$ protons in sperm whale skeletal and horse heart myoglobins have been located for the first time in the downfield shifted portion of the spectra. The shifts and hydrogen exchange rates indicate that these His imidazole ring NH protons are involved in the inter-segmental hydrogen bonds of the protein in solution, as demonstrated by a crystallographic study [Takano, T. (1977) *J. Mol. Biol.* 220, 381-399]. The assigned His imidazole ring NH proton resonances can serve as new sensitive structural probes in the study of the local conformation of myoglobin. The applicability of the NMR spectral parameters in the study of the tertiary structure of apomyoglobin, the denaturation of the protein, and the protein stability of sperm whale and horse myoglobins is presented in some detail.

Key words: apomyoglobin, hydrogen bond, myoglobin, NMR, protein folding.

Myoglobin (Mb) is a monomeric b-type hemoprotein of ~17 kDa and consists of eight helices, A through H, that are linked by short polypeptide segments to form an oblate spheroidal molecule. In spite of a subtle argument as to the importance of internal hydrogen bonds in stabilization of the structure of a native protein relative to its unfolded state, internal hydrogen bonds provide a structural basis for its native folding pattern (*1*). A crystallographic study of Mb revealed many internal hydrogen bonds between the side-chains of hydrophilic amino acid residues, that were proposed to stabilize the tertiary structure of the protein (*2, 3*). These internal hydrogen bonds can be used as sensitive probes for characterizing the local structure of the protein. ^{1}H NMR permits direct observation of the signals arising from protons involved in such internal hydrogen bonds.

^{1}H resonance assignment for the diamagnetic carbonmonoxy form of sperm whale Mb [Mb(CO)] has been extensively performed by Wright and co-workers (*4-6*). ^{1}H resonances arising from 95% of the amino acid residues in this Mb have been assigned by means of the nuclear Overhauser effect (NOE)-based sequential assignment procedure using uniformly ^{15}N-labeled Mb (*6*). Although the site-specific titration behaviors of twelve His residues in sperm whale Mb have been analyzed in detail on the basis of the pH dependence of the shifts for His imidazole ring non-exchangeable CH proton resonances (*7*) in order to determine the electronic environments around the individual residues, His imidazole ring NH proton resonances have not been located except for that of HisF8 $N_\delta H$ (*6*). In general, these labile proton resonances are quite elusive and not always observable due to a rapid hydrogen exchange process. However, when they are buried in the protein matrix and involved in internal hydrogen bonds, their moderate exchange and magnetically deshielded environments enable one to observe their NMR resonances in the downfield shifted region of the spectra (*8*). In the present study, we focused on observation of the ^{1}H NMR signals arising from such His ring NH protons in Mb, which are thought to constitute new sensitive structural probes for the study of the tertiary structure of this protein, because of their remarkable sensitivity to the electronic and structural properties of the environments (*9*).

We report herein the observation of three ^{1}H NMR signals arising from His imidazole ring NH protons in the downfield shifted region of the spectra of sperm whale and horse Mb(CO)s. Two signals have been assigned to the HisB5 $N_\delta H$ and HisEF5 $N_\epsilon H$ protons on the basis of comparison of the spectra with those of apomyoglobin (apoMb), and shark (*Galeorhinus japonicus*) and mollusc (*Dolabella auricularia*) Mb(CO)s and NOE connectivities. Their hydrogen exchange rates of $\ll 3\times10^3$ s^{-1}, estimated from their resonance frequencies, strongly support that they are involved in internal hydrogen bonds. These results are consistent with the crystal structure, which revealed the presence of hydrogen bonds between AspB1 and HisB5, and between HisEF5 and AspH18 (*2, 3*). These hydrogen bonds in apoMb and their stability against an added denaturant, guanidine hydrochloride (Gdn-HCl), are inferred from NMR spectral parameters of the His imidazole ring NH proton signals. The potential applicability of the assigned resonances to the structural characterization of Mb and apoMb is discussed.

MATERIALS AND METHODS

Sperm whale skeletal and horse heart Mbs were purchased from Biozyme and Sigma Chemical, respectively, and used without further purification. Shark (*Galeorhinus japonicus*) Mb was extracted from red muscle and purified as previously reported (*10*). Mollusc Mb was extracted from the triturative stomach of *Dolabella auricularia* and purified as reported (*11*). The carbonmonoxy form of the protein was

[1] Phone & Fax: +81-298-53-6925, e-mail: yash@sakura.cc.tsukuba.ac.jp

Abbreviations: Mb, myoglobin; Mb(CO), carbonmonoxy myoglobin; NOE, nuclear Overhauser effect; apoMb, apomyoglobin; Gdn-HCl, guanidine hydrochloride.

prepared by the injection of CO gas and the addition of sodium dithionite (Kanto Chemical). Guanidine hydrochloride was purchased from Wako Chemicals. The concentration of the protein in NMR samples was about 0.5 mM in 90% H_2O/10% ^2H_2O. The pH of the sample was adjusted using 0.2 M NaOH or 0.2 M HCl, and the value was measured with a Horiba F-22 pH meter with a Horiba type 6069-10C electrode. The NMR spectra were recorded with a Bruker AC-400P FT NMR spectrometer operating at the ^1H frequency of 400 MHz. The spectra were recorded with 1k transients, a spectral width of 15 kHz, 8k data points and a recycle time of 1 s. The nuclear Overhauser effect (NOE) was observed by selectively saturating a desired peak for 100 ms, and the results are presented in the form of NOE difference spectra. Chemical shifts are given in ppm downfield from sodium 2,2-dimethyl-2-silapentane-5-sulfonate with the residual H^2HO as an internal reference.

RESULTS

NMR Signals Arising from His Imidazole Ring NH Protons in Various Mb(CO)s and Their Assignments—The downfield portion of the 400 MHz ^1H NMR spectrum of sperm whale carbonmonoxy Mb [Mb(CO)] in 90% H_2O/10% ^2H_2O, pH 8.22, at 5°C is presented as spectrum A of Fig. 1. Three signals, peaks a-c, are observed in this region. The absence of these peaks in the spectrum of the 100% ^2H_2O sample (result not shown) indicates that they arise from exchangeable protons. The difference in the resonance frequency between these signals and the bulk water signal dictates that their hydrogen exchange rates should be $\ll 3 \times 10^3\ s^{-1}$. The shifts and hydrogen exchange rates of these protons resemble those of a His imidazole ring NH proton or Trp indole NH proton, which is buried in the protein matrix and possibly involved in an internal hydrogen bond (*8, 9, 12*). The reported assignments for the HisF8 $N_\delta H$ proton signal and the indole NH proton signals for all the Trp residues in sperm whale Mb(CO) (*6*) preclude these protons from being candidates for the assignments of peaks a-c. Their temperature dependence is illustrated in A of Fig. 2. A slight upfield shift and considerable exchange broadening are observed for all the signals with increasing temperature. The pH dependence shown in Fig. 2B reflects their characteristic exchange behaviors. In a slow exchange regime such as that observed in the present case, the line width of a labile proton signal increases with increasing the exchange rate. Hence the broadening of peaks a and c under acidic and basic pH conditions, observed in Fig. 2B, is attributed to acid and base catalyses in their exchange, with the minimum rate at pH ~8. On the other hand, peak b shows acid catalysis and strong resistance to base catalysis in its exchange. These results are also consistent with their assignment to His ring NH protons involved in hydrogen bonds (for proton b, see below).

The assignment of these signals to specific His residues can be made with the spectral comparison with those of sperm whale apomyoglobin (apoMb), and horse, shark (*G. japonicus*), and mollusc (*D. auricularia*) Mb(CO)s. Removal of heme from whale Mb results in spectrum A′ in Fig. 1. In the absence of the heme, peak c disappears completely from the spectrum, and peaks a and b are slightly shifted downfield relative to the corresponding signals in trace 1A. Besides HisF8, HisFG3 is the only residue which directly interacts with heme in Mb; the HisFG3 $N_\epsilon H$ proton is hydrogen-bonded to heme 7-propionate O_δ (*2, 3*). The heme extraction leads to the abolition of this HisFG3-heme hydrogen bond, which in turn results in great acceleration of the chemical exchange of the HisFG3 $N_\epsilon H$ proton. Consequently, peak c is likely to arise from the HisFG3 $N_\epsilon H$ proton. Horse Mb possesses ten His residues besides HisF8, and its spectrum is quite similar to spectrum 1A, although the separation of peaks b and c in the spectrum is obscure due to exchange line broadening. The slight difference in spectral parameters between the corresponding signals of whale and horse Mb(CO)s reflects a sizable difference in the chemical environments of the protons between the proteins. Two exchangeable proton signals are observed in the spectrum of shark Mb(CO) (trace 1C), and their temperature and pH dependence is similar to that of

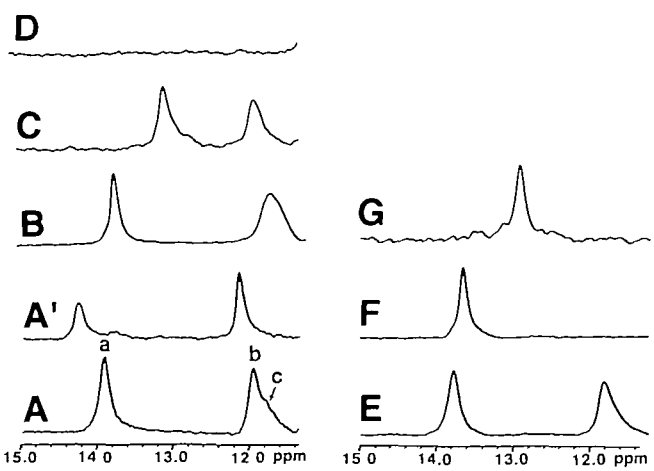

Fig. 1. **The downfield portions of the 400 MHz ^1H NMR spectra of various Mb(CO)s in 90% H_2O/10% ^2H_2O.** (A), (E) sperm whale Mb(CO), pH 8.22; (A′) sperm whale apoMb, pH 9.48; (B), (F) horse heart Mb(CO), pH 8.62; (C), (G) shark (*Galeorhinus japonicus*) Mb(CO), pH 8.75; (D) mollusc (*Dolabella auricularia*) Mb(CO), pH 8.55. (A)-(D) and (A′) were recorded at 5°C and (E)-(G) at 25°C. Peaks a-c arise from His imidazole ring NH protons.

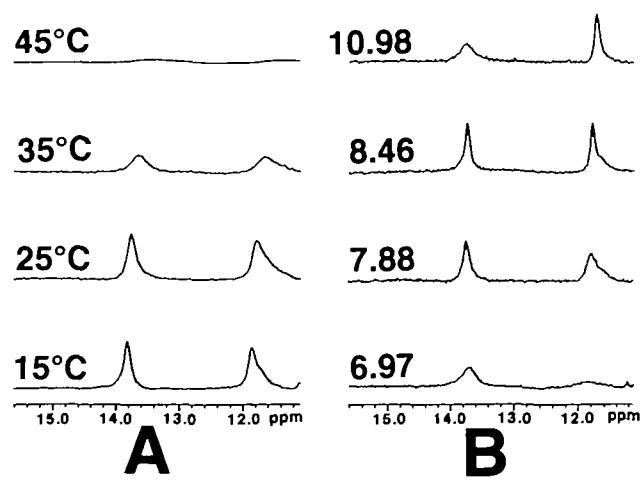

Fig. 2. **(A) The downfield portions of ^1H NMR spectra of sperm whale Mb(CO) in 90% H_2O/10% ^2H_2O, pH 8.02, at the indicated temperatures, and (B) the spectra of sperm whale Mb(CO) in 90% H_2O/10% ^2H_2O at 25°C and the indicated pH values.**

peaks a and c in trace 1A. Among the four His residues in this shark Mb, three appear to occupy the same helical positions as those in both horse and whale Mbs, and they are HisEF5, HisF8, and HisFG3 (*10, 13*). The signal arising from the HisF8 $N_\delta H$ proton in Mb(CO)s has shown to resonate at ~9.5 ppm (*5, 14*), and therefore two peaks in trace 1C are attributable to the imidazole ring NH protons of HisEF5 and HisFG3. Since, as described above, peak c is tentatively assigned to the HisFG3 $N_\epsilon H$ proton, peak a is attributed to the His EF5 imidazole NH proton. In fact, according to the X-ray structures of sperm whale (*2*) and horse (*15, 16*) Mbs, this residue is one of the most highly buried His residues in the protein [the solvent exposure of this His residue in whale Mb is estimated to be 0.048 nm^2 (*17*)]. An X-ray study demonstrated that the $N_\epsilon H$ proton of HisEF5 is hydrogen-bonded to O_δ of AspH18, and this internal hydrogen bond was proposed to stabilize the interface between the EF corner and the H helix (*2*). The assignment of peak a to the HisEF5 $N_\epsilon H$ proton is completely consistent with our previous result (*18*). For the assignment of peak b, HisB5 and HisGH1 are likely to be selected as candidates. These two His residues are highly buried in the protein matrix [the solvent exposure of HisB5 and HisGH1 is 0.028 and 0.165 nm^2, respectively (*17*)], and are involved in a unique internal hydrogen bond, *i.e.* the $N_\epsilon H$ proton of HisGH1 is hydrogen-bonded to N_ϵ of HisB5, and the $N_\delta H$ proton of HisB5 interacts with the peptide carbonyl oxygen of AspB1 (*2, 15, 16*). This internal hydrogen bond was proposed to stabilize the interface between the B helix and the GH corner. Finally, the absence of signals in the spectrum of mollusc Mb(CO) (trace 1D), possessing a single His residue at the helical position of F8 (*11*), also supports that the signals observed in the spectra in Fig. 1 arise from His imidazole ring NH protons.

Further assignments can be derived through the observation of NOE connectivities. NOE difference spectra recorded for whale Mb(CO) in 90% H_2O/10% ^2H_2O, pH 8.46, at 35°C are shown in Fig. 3. As can be seen in trace B, irradiation of the HisEF5 $N_\epsilon H$ proton signal yields almost equivalent NOEs to two peaks at 6.54 and 7.46 ppm. These shifts are quite similar to those of the HisEF5 $C_\delta H$ and $C_\epsilon H$ protons (6.69 and 7.63 ppm, respectively) reported for the same protein at 35°C and pH 5.6 (*6*), which are located at 0.28 and 0.23 nm, respectively, away from the $N_\epsilon H$ proton. Furthermore, the NOE difference spectra observed at different pH values, 6.5–9, indicate that their shifts are essentially independent of pH. This result is also consistent with the absence of pH-dependent shifts for the $C_\epsilon H$ and $C_\delta H$ proton resonances of HisEF5 (*7, 14*). As can be seen in trace C in Fig. 3, irradiation of the signal at 11.69 ppm yields NOEs to two peaks at 7.47 and 7.61 ppm, which also exhibit no significant pH-dependent shift changes at 6.5–9. Their shifts are similar to the reported values for the HisB5 amido NH and imidazole ring $C_\epsilon H$ protons, 7.56 and 7.91 ppm, respectively (*6*), which are located at 0.25 and 0.27 nm, respectively, away from the HisB5 $N_\delta H$ proton. The difference of 0.3 ppm for the $C_\epsilon H$ proton shift could be attributed to a pH effect. Although pK_a for HisB5 has shown to be <4.8 (*14*), the electronic structure of the imidazole ring of this residue could be modulated by pH through the interacting HisGH1, whose pK_a is 6.1 (*7*). Additionally, the intensity of the signal at 7.47 ppm in the NOE difference spectra was found to be influenced by the solvent composition ($H_2O/^2H_2O$), indicating that this signal arises from an exchangeable proton. Consequently, these results are consistent with the assignment of the peak at 11.69 ppm to the HisB5 $N_\delta H$ proton. The observation of these His imidazole ring NH proton resonances provides direct evidence that these internal hydrogen bonds in these proteins are formed in solution.

The spectra of whale, horse and shark Mb(CO)s recorded at 25°C are shown as traces E–G in Fig. 1, respectively. The signal tentatively assigned to the HisFG3 $N_\epsilon H$ proton (peak c) has disappeared from the spectrum. This result might be

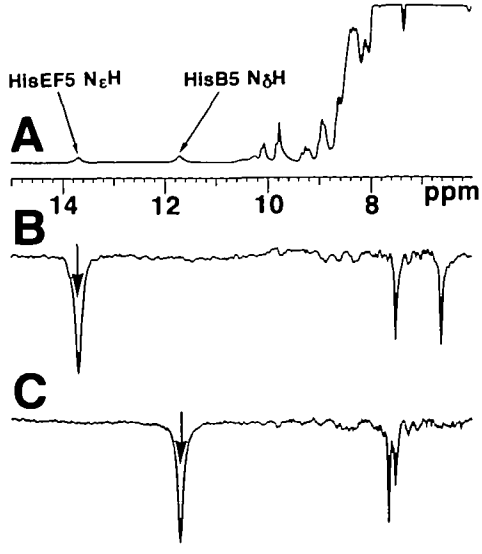

Fig. 3. **(A) The downfield portions of ^1H NMR spectra of sperm whale Mb(CO) in 90% H_2O/10% ^2H_2O, pH 8.46, at 35°C. (B) The NOE difference spectrum resulting from saturation of the HisEF5 $N_\epsilon H$ proton signal.** The peaks at 6.54 and 7.46 ppm exhibit NOEs. **(C) The NOE difference spectrum resulting from saturation of an exchangeable peak at 11.69 ppm, *i.e.* that of the HisEF5 $N_\epsilon H$ proton.** The peaks at 7.47 and 7.61 ppm exhibit NOEs. In (B) and (C), an arrow indicates the peak saturated with a decoupler pulse.

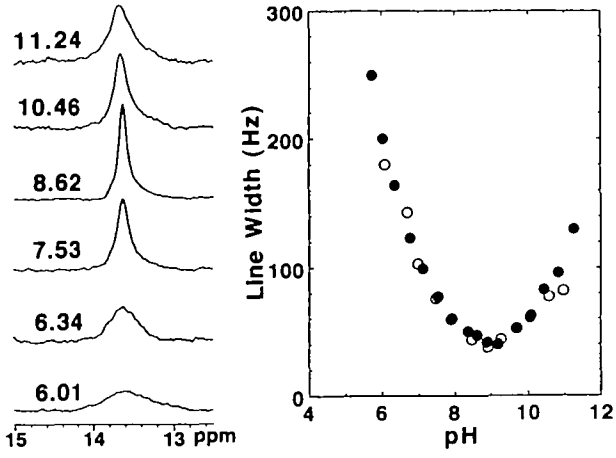

Fig. 4. **The signals of the HisEF5 $N_\epsilon H$ proton of horse Mb(CO) in 90% H_2O/10% ^2H_2O at 25°C and the indicated pH (left), and plots of the line width for the signals of horse (filled circles) and sperm whale (open circles) Mb(CO)s as a function of pH (right).**

due to the fact that the HisFG3 residue is relatively exposed to the solvent [its solvent exposure in whale Mb was calculated to be 0.799 nm^2 (*17*), although its $N_\epsilon H$ proton is hydrogen-bonded to a carboxyl oxygen of the heme 7-propionate group]. In addition, the signal for the HisB5 $N_\delta H$ proton in whale Mb(CO) is observed at 25°C, whereas that in horse Mb(CO) has disappeared completely. The difference in the line broadening behavior of the HisB5 $N_\delta H$ proton signal between these two Mb(CO)s indicates that, at a given temperature, the hydrogen exchange rate for this proton in the former is substantially larger than that in the latter. This result is interpreted in terms of the difference in stability of the protein structure between them (see below).

pH Dependence of the HisEF5 $N_\epsilon H$ Proton Signal—The pH dependence of the HisEF5 $N_\epsilon H$ proton signal of horse Mb(CO) at 25°C is shown in Fig. 4, and a plot of its line width against pH, together with the same plot for the corresponding signal in whale Mb(CO), for comparison, is also illustrated in the figure. In contrast with the large difference in the exchange rate for the HisB5 $N_\delta H$ proton between the two Mbs, the plots in Fig. 4 demonstrate that the hydrogen exchange rate for the HisEF5 $N_\epsilon H$ proton in these proteins is essentially identical over a wide pH range. Since the hydrogen exchange rate of a labile proton is related to the strength of the hydrogen bond or/and the accessibility of the proton to the solvent, the present results indicate that the AspB1-HisB5 hydrogen bond in whale Mb(CO) is more stable than that in horse Mb(CO), whereas the strengths of the HisEF5-AspH18 hydrogen bonds in these two Mbs are similar. These results strongly suggest that the structural stability of one part of Mb is independent of that of other parts within a molecule.

Effects of a Denaturant on the His Imidazole Ring NH Proton Signals—The spectra of sperm whale Mb(CO) in the presence of different concentrations of a common denaturant for proteins, guanidine hydrochloride (Gdn-HCl), are illustrated in Fig. 5. At the Gdn-HCl concentration of 2 M, the electronic spectrum of sperm whale Mb(CO) indicated that the Soret band at 417 nm remains at 80% relative intensity, and at the concentration of 6 M, the protein appeared to be completely unfolded (results not shown). Both the HisEF5 $N_\epsilon H$ and HisB5 $N_\delta H$ proton signals are shifted upfield and considerably broadened with increasing concentrations of Gdn-HCl. But there is a clear difference in the perturbation induced by the denaturant between the two signals. Additionally, the signals arising from other imidazole ring protons, *i.e.*, HisB5 $C_\delta H$, and HisEF5 $C_\delta H$ and $C_\epsilon H$ protons, observed in NOE difference spectra, shift only slightly (~0.1 ppm) upfield with increasing concentrations of Gdn-HCl (results not shown).

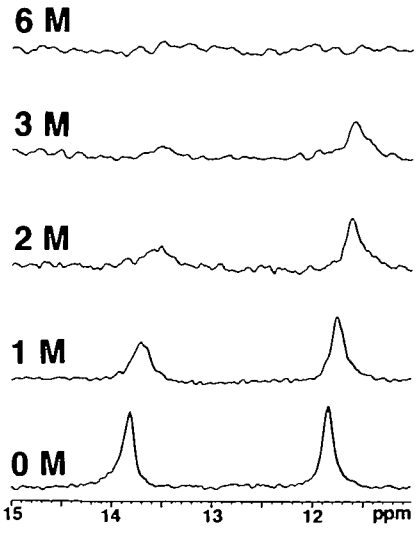

Fig. 5. **The downfield portions of the 400 MHz ^1H NMR spectra of sperm whale Mb(CO) in 90% H_2O/10% D_2O, pH 8.65, at 25°C in the presence of the indicated concentrations of guanidine hydrochloride.** The signals shifted upfield and became broadened with increasing concentration of the denaturant.

DISCUSSION

Interface between the EF Corner and the H Helix—Crystallographic studies of whale and horse Mbs revealed that the HisEF5 $N_\epsilon H$ proton is hydrogen bonded to O_δ of AspH18 (*2, 3, 15, 16*). The present study clearly indicated that this inter-segmental hydrogen bond is formed in these Mbs in solution. Furthermore, in spite of the low sequence homology (~40%) between the shark and mammalian Mbs, the observation of the signal for the HisEF5 $N_\epsilon H$ proton in the spectra of shark Mb(CO) revealed that the HisEF5-AspH18 hydrogen bond is also present in this Mb. The difference in the shift of the HisEF5 $N_\epsilon H$ proton signal between the proteins suggests a possible difference in the hydrogen-bonding interaction between HisEF5 and AspH18. However, the similarity in the chemical exchange behavior of the HisEF5 $N_\epsilon H$ proton, as reflected in the pH dependence of the line width shown in the plots in Fig. 4, between whale and horse Mb(CO)s strongly suggests that the chemical environments around this proton in these two proteins are highly alike. The conformational similarity of the EF-H interface in the two Mbs is consistent with the results of comparative studies of their X-ray structures (*15, 16*).

As shown in the spectra in Fig. 4, the shift of the HisEF5 $N_\epsilon H$ proton signal is essentially independent of the pH value, 6-11, indicating that the HisEF5-AspH18 hydrogen bond is not significantly altered under these pH conditions. But the exchange line broadening demonstrates that the hydrogen exchange of this proton reflects both acid and base catalyses.

AspB1-HisB5 Hydrogen Bond—The observation of the HisB5 $N_\delta H$ proton signal in horse and whale Mb(CO)s revealed that this proton is hydrogen-bonded to a peptide carbonyl oxygen of AspB1, as demonstrated by the X-ray structure (*2*). However, although the conformation of the segment, AspB1-HisB5, in whale and horse Mbs is quite similar in the crystalline state, a difference being in the side chain of the B2 residue, Val in whale Mb being replaced by Ile in horse Mb (*15, 16*), the chemical exchange rate of the HisB5 $N_\delta H$ proton was found to be substantially different between the two Mbs. For a proposed unique triad hydrogen-bonding network, AspB1-HisB5-HisGH1 (*2, 3*), the formation of the HisB5-HisGH1 hydrogen bond in these proteins in solution has been confirmed by the inter-residue NOE connectivities (*5, 19, 20*). An X-ray study has further revealed significant differences in the secondary structure at the GH corner between the two Mbs, where residues ProGH2 to PheGH5 in whale Mb form a distorted type I

reverse turn, whereas a type II turn is present at residues HisGH1 to AspGH4 in horse Mb (*15, 16*). The present data suggest that such a local conformational change, together with the differences in the hydrogen-bond network, as shown in Fig. 6, affects the AspB1-HisB5 hydrogen bond. In fact, the distance between HisB5 N_δ and the peptide carbonyl oxygen of AspB1 in whale Mb in the crystalline state is about 0.03 nm smaller than that in horse Mb, and the distance between the N_ϵ atoms of HisB5 and HisGH1 in whale Mb is slightly smaller than that in horse Mb (*2, 15, 16*). Hence the polarization of the two N-H bonds in this unique triad hydrogen-bond network might be correlated through the electronic interaction across the two imidazole rings. In such a case, the strength of the HisB5-HisGH1 hydrogen bond could be inferred on analysis of the AspB1-HisB5 hydrogen bond.

Under acidic pH conditions, the HisGH1 imidazole ring in whale Mb is protonated with a pK_a of 6.1 (*7*), and then the proton between the N_ϵ atoms of two His residues, B5 and GH1, was proposed to migrate from one imidazole to the other, resulting in delocalization of the positive charge in the protein matrix (*17*). Therefore, acid catalysis is expected for the hydrogen exchange of the HisB5 $N_\delta H$ proton. On the other hand, strong resistance to base catalysis for the exchange of this proton can be rationalized by the fact that, in addition to the AspB1-HisB5 hydrogen bond, the N_ϵ atom of HisB5 is blocked by another hydrogen bond with the HisGH1 $N_\epsilon H$ proton.

Tertiary Structure of apoMb—Removal of heme renders apoMb less stable than Mb, and reduces its helical content. The structural characterization of apoMb has been extensively performed (*14, 19-28*). However, the regions of Mb that are substantially affected by heme extraction have not been fully identified. A solution NMR study has revealed that the A, B, G, and H helices in apoMb maintain the same packing as they do in Mb (*22*). The present study revealed that the AspB1-HisB5 and HisEF5-AspH18 hydrogen bonds survive heme extraction. The presence of the AspB1-HisB5 hydrogen bond is completely consistent with the previous finding (*22*). Additionally, the stabilization of the EF corner by the HisEF5-AspH18 hydrogen bond, together with the formation of the G helix, strongly sug-

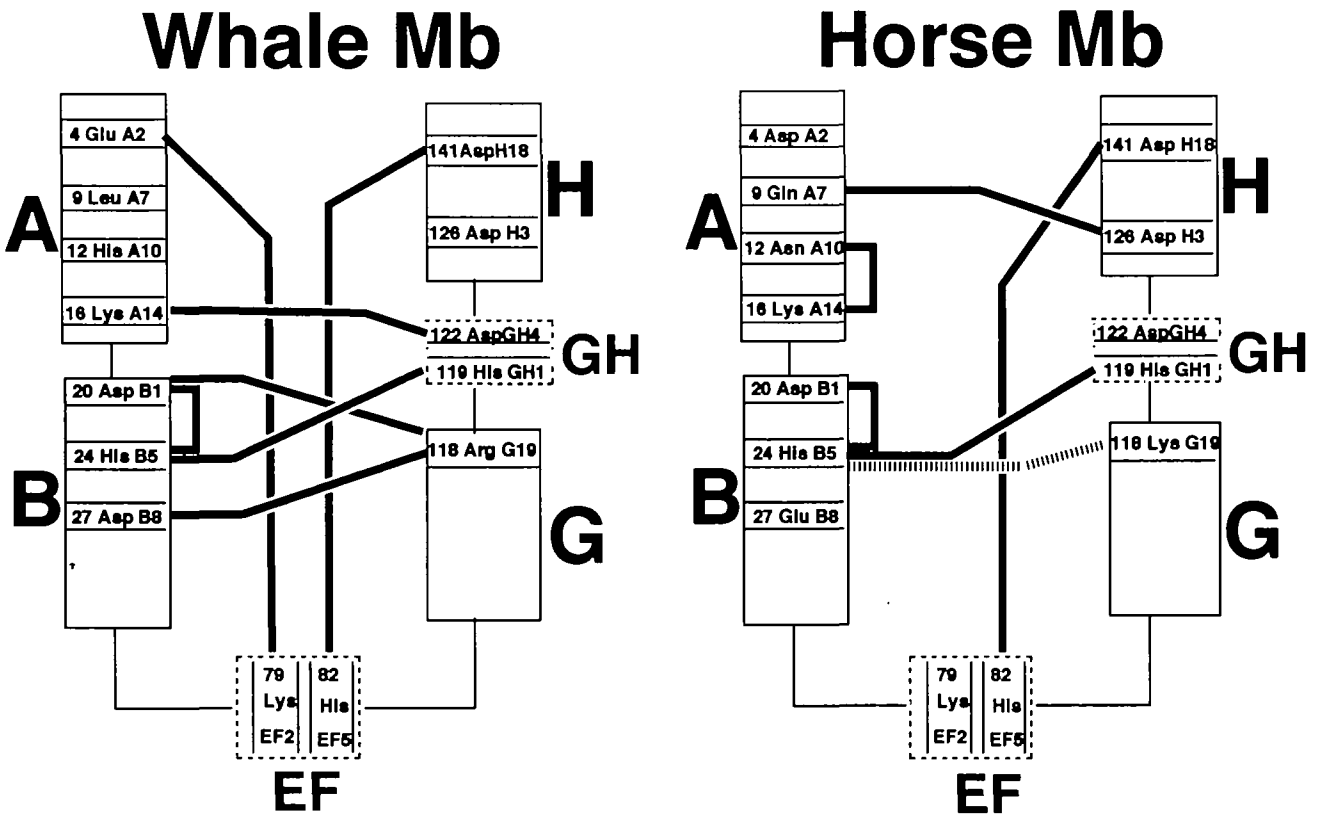

Fig. 6. **The internal hydrogen-bond network in the hydrophobic core composed of the A, B, G, and H helices in sperm whale and horse Mbs (*2, 3, 15, 16*).** In the figure, the helices are indicated by rectangles. The rectangles with broken lines, EF and GH, represent non-helical segments between corresponding helices. The internal hydrogen bonds are indicated by thick lines connecting two interacting amino acid residues. Due to the substitution of five amino acid residues in this region, these Mbs exhibit considerably different hydrogen-bond patterns. The replacement of GluA2, which forms a salt bridge with LysEF2 in whale Mb, by Asp in horse Mb leads to the loss of the specific interaction at the A-EF interface, resulting in alteration of the N-terminal structure of the protein. The replacement of LeuA7 in whale Mb for Gln in horse Mb leads to the formation of a new GlnA7-AspH3 salt bridge. The replacement of HisA10 in whale Mb by Asn in horse Mb results in the loss of the LysA14-AspGH4 salt bridge found in whale Mb and the formation of an AsnA10-LysA14 salt bridge in horse Mb. Finally, the substitution of a pair of amino acid residues, *i.e.*, AspB6 to Glu and ArgG19 to Lys, results in the loss of the hydrogen bonds between AspB1 and ArgG19, and AspB8 and ArgG19 observed in whale Mb, in favor of forming the AspB1-HisB5 hydrogen bond, together with possible hydrogen bond formation between HisB5 and LysG19, in horse Mb. The HisB5-HisGH1 and HisEF5-AspH18 hydrogen bonds are found in both proteins. A hydrogen bond between HisB5 and LysG19 in horse Mb has been proposed (*15, 16*).

gests that the F helix in apoMb is at least partly folded. Hence the reduced helicity in apoMb, relative to that in Mb, would be largely due to the unfolding of the C-E helices. Careful scrutiny of the tertiary structure of apoMb in solution, using the assigned His resonances as structural probes, is underway in our laboratory.

Effects of Gdn-HCl on the HisB5 $N_\delta H$ and His EF5 $N_\epsilon H$ Proton Resonances—The folding of small globular proteins such as Mb generally proceeds cooperatively under physiological conditions (*23*). Although the characterization of partly folded intermediates is expected to provide a detailed description of the folding process, they are rarely observed due to, mainly, their short life-times. On the other hand, the unfolding transitions induced by a variety of denaturants for proteins have been analyzed thoroughly, and such studies have provided a wealth of information on the folding of proteins (*21-25, 27-36*). However, since the denaturation of proteins is usually monitored by means of spectrophotometric techniques or thermal analysis (*21-25, 29-36*), the effect of a denaturant on the tertiary structure of a protein molecule has not been fully investigated.

Since alteration of the electronic structure of either a hydrogen-donor or -acceptor leads to shift changes in these resonances, the denaturant-dependent shifts, observed in Fig. 5, cannot be interpreted solely in terms of the strength of the hydrogen-bonding interaction. But the induced upfield-shift on the addition of the denaturant is consistent with weakening of the hydrogen bond, which results in decreasing magnitude of the polarization of the N-H bond. The fact that the other imidazole ring proton signals for these two His residues shift only slightly on the addition of Gdn-HCl also supports this interpretation. Moreover, the broadening of the signals indicates that the hydrogen exchange rates for these protons increase with the concentration of the denaturant. As mentioned above, the accelerated exchange rate is attributed to the weakening of the hydrogen bond. Consequently, both the changes in the shifts and line widths of these His ring $N_\epsilon H$ proton signals, induced by the denaturant, are consistent with the alteration of the AspB1-HisB5 and HisEF5-AspH18 hydrogen bonds. Consequently, it is concluded from the spectral alterations in Fig. 5 that the HisEF5-AspH18 hydrogen bond is more susceptible to Gdn-HCl than the AspB1-HisB5 one, although it is not clear at present if the denaturant directly attacks this particular site of a molecule. The greater susceptibility of the HisEF5-AspH18 hydrogen bond to Gdn-HCl than that of the AspB1-HisB5 one in the protein could be rationalized by the fact that the former contributes to stabilization of the tertiary structure of the protein, whereas the latter appears to be used in reinforcing the formation of the B-helix, which has shown to be one of the helices involved in the relatively stable hydrophobic core in Mb (*22*). Slight alteration of the protein folding could result in a sizable conformational alteration of the EF-H interface.

Protein Stability of Whale and Horse Mbs—Regarding their structure-function relationships, the differences in conformational stability (*37-39*) and kinetic behaviors (*40, 41*), although they are essentially isostructural with each other (*15, 16*), remain to be explained. The previous attempts to correlate the different stabilities of these two highly homologous proteins as to various structural parameters of the molecules did not lead to any conclusive interpretation (*37, 38*). ^{1}H NMR studies of apomyoglobin have shown that the A, B, G, and H helices form hydrophobic cores in the protein, which was proposed to be important for the protein stability (*19, 20, 23*). The internal hydrogen bond networks inside the core in the two Mbs are compared in Fig. 6. The present study demonstrated that the AspB1-HisB5 hydrogen bond in whale Mb is substantially stronger than that in horse Mb. The effects of Gdn-HCl on the assigned His NH proton resonances revealed that the AspB1-HisB5 hydrogen bond is more resistant against the denaturant than the HisEF5-AspH18 one. The observed difference in the stability of the AspB1-HisB5 hydrogen bond between whale and horse Mbs could be directly related to the lower stability of the former protein. This correlation strongly suggests that the B-GH interface is crucial to the thermodynamic stability of Mb. But the value of 10.9 kJ/mol for the difference in the conformational free energy of unfolding between the two Mbs (*37-39*) is too large to be only accounted for by a difference in the stabilization energy for a single internal hydrogen bond. Hence the stabilization by other interactions also needs to be considered when interpreting the overall stability of the proteins.

The author wishes to thank Dr. Tomohiko Suzuki (Kochi University) for the shark and mollusc Mbs.

REFERENCES

1. Voet, D. and Voet, J.G. (1991) *Biochemistry*, Chapter 7, Wiley, New York
2. Takano, T. (1977) Structure of myoglobin refined at 2.0 Å resolution. I. Crystallographic refinement of metmyoglobin from sperm whale. *J. Mol. Biol.* **110**, 537-568
3. Cheng, X. and Schoenborn, B.P. (1991) Neutron diffraction study of carbonmonoxymyoglobin. *J. Mol. Biol.* **220**, 381-399
4. Mabbutt, B.C. and Wright, P.E. (1985) Assignment of heme and distal amino acid resonances in the ^{1}H-NMR spectra of the carbon monoxide and oxygen complexes of sperm whale myoglobin. *Biochim. Biophys. Acta* **832**, 175-185
5. Dalvit, C. and Wright, P.E. (1987) Assignment of resonances in the ^{1}H nuclear magnetic resonance spectrum of the carbon monoxide complex of sperm whale myoglobin by phase-sensitive two-dimensional techniques. *J. Mol. Biol.* **194**, 313-327
6. Thériault, Y., Pochapsky, T.C., Dalvit, C., Chiu, M.L., Sligar, S.G., and Wright, P.E. (1994) ^{1}H and ^{15}N resonance assignments and secondary structure of the carbon monoxide complex of sperm whale myoglobin. *J. Biomol. NMR* **4**, 491-504
7. Bashford, D., Case, D.A., Dalvit, C., Tennant, L., and Wright, P.E. (1993) Electrostatic calculations of side-chain pK_a values in myoglobin and comparison with NMR data for histidines. *Biochemistry* **32**, 8045-8056
8. Robillard, G. and Shulman, R.G. (1972) High resolution nuclear magnetic resonance study of the histidine-aspartate hydrogen bond in chymotrypsin and chymotrypsinogen. *J. Mol. Biol.* **71**, 507-511
9. Markley, J. (1975) Observation of histidine residues in protein by nuclear magnetic resonance spectroscopy. *Acc. Chem. Rec.* **8**, 70-80
10. Suzuki, T., Suzuki, T., and Yata, T. (1985) Shark myoglobins. II. Isolation, characterization and amino acid sequence of myoglobin from *Galeorhinus japonicus*. *Aust. J. Biol. Sci.* **38**, 347-354
11. Suzuki, T. (1986) Amino acid sequence of myoglobin from the mollusc *Dolabella auricularia*. *J. Biol. Chem.* **261**, 3692-3699
12. Wüthrich, K. (1986) *NMR of Proteins and Nucleic Acids*, John Wiley & Sons, New York
13. Suzuki, T. (1987) Autoxidation of oxymyoglobin with the distal(E7) glutamine. *Biochim. Biophys. Acta* **914**, 170-176

14. Cocco, M., Kao, Y.-H., Phillips, A.T., and Lecomte, J.T.J. (1992) Structural comparison of apomyoglobin and metaquomyoglobin: pH titration of histidines by NMR spectroscopy. *Biochemistry* **31**, 6481-6491
15. Evans, S.V. and Brayer, G.D. (1988) Horse heart metmyoglobin. A 2.8 Å resolution three-dimensional structure determination. *J. Biol. Chem.* **263**, 4263-4268
16. Evans, S.V. and Brayer, G.D. (1990) High-resolution study of the three-dimensional structure of horse heart metmyoglobin. *J. Mol. Biol.* **213**, 885-897
17. Barrick, D., Hughson, F.M., and Baldwin, R.L. (1994) Molecular mechanisms of acid denaturation. The role of histidine residues in the partial unfolding of apomyoglobin. *J. Mol. Biol.* **237**, 588-601
18. Yamamoto, Y. and Suzuki, T. (1996) NMR study of the active site of shark met-cyano myoglobin. *Biochim. Biophys. Acta* **1293**, 129-139
19. Lecomte, J.T.J. and Cocco, M.J. (1990) Structural features of the protoporphyrin-apomyoglobin complex: A proton NMR spectroscopy study. *Biochemistry* **29**, 11057-11067
20. Cocco, M.J. and Lecomte, J.T.J. (1990) Characterization of hydrophobic cores in apomyoglobin: A proton NMR spectroscopy study. *Biochemistry* **29**, 11067-11072
21. Griko, Y.V., Privalov, P.L., Venyaminov, S.Y., and Kutyshenko, V.P. (1988) Thermodynamic study of the apomyoglobin structure. *J. Mol. Biol.* **202**, 127-138
22. Hughson, F.M. and Baldwin, R.L. (1989) Use of site-directed mutagenesis to destabilize native apomyoglobin relative to folding intermediates. *Biochemistry* **28**, 4415-4422
23. Hughson, F.M., Wright, P.E., and Baldwin, R.L. (1990) Structural characterization of a partly folded apomyoglobin intermediate. *Science* **249**, 1544-1548
24. Jennings, P.A. and Wright, P.E. (1993) Formation of a molten globule intermediate early in the kinetic folding pathway of apomyoglobin. *Science* **262**, 892-896
25. Barrick, D. and Baldwin, R.L. (1993) Three-state analysis of sperm whale apomyoglobin folding. *Biochemistry* **32**, 3790-3796
26. Lin, L., Pinker, R.J., Forde, K., Rose, G.D., and Kallenbach, N.R. (1994) Molten globular characteristics of the native state of apomyoglobin. *Nature Struct. Biol.* **1**, 447-452
27. Loh, S.N., Kay, M.S., and Baldwin, R.L. (1995) Structure and stability of a second molten globule intermediate in the apomyoglobin folding pathway. *Proc. Natl. Acad. Sci. USA* **92**, 5446-5450
28. Kataoka, M., Nishi, I., Fujisawa, T., Ueki, T., Tokunaga, F., and Goto, Y. (1995) Structural characterization of the molten globule and native states of apomyoglobin by solution X-ray scattering. *J. Mol. Biol.* **249**, 215-228
29. Pace, C.N. and Vanderburg, K.E. (1979) Determining globular protein stability: Guanidine hydrochloride denaturation of myoglobin. *Biochemistry* **18**, 288-291
30. Pace, C.N. (1986) Determination and analysis of urea and guanidine hydrochloride denaturation curves. *Methods Enzymol.* **131**, 266-289
31. Privalov, P.L., Griko, Y.V., Venyaminov, S.Y., and Kutyshenko, V.P. (1986) Cold denaturation of myoglobin. *J. Mol. Biol.* **190**, 487-498
32. Goto, Y. and Fink, A.L. (1990) Phase diagram of acidic conformational states of apomyoglobin. *J. Mol. Biol.* **214**, 803-805
33. Hagihara, Y., Amino, S., Fink, A.L., and Goto, Y. (1993) Guanidine hydrochloride-induced folding of proteins. *J. Mol. Biol.* **231**, 180-184
34. Griko, Y.V. and Privalov, P.L. (1994) Thermodynamic puzzle of apomyoglobin unfolding. *J. Mol. Biol.* **235**, 1318-1325
35. Nishi, I., Kataoka, M., and Goto, Y. (1995) Thermodynamic stability of the molten globule states of apomyoglobin. *J. Mol. Biol.* **250**, 223-238
36. Kiefhaber, T. and Baldwin, R.L. (1995) Intrinsic stability of individual α helices modulates structure and stability of the apomyoglobin molten globule form. *J. Mol. Biol.* **252**, 122-132
37. Puett, D. (1973) The equilibrium unfolding parameters of horse and sperm whale myoglobin. *J. Biol. Chem.* **248**, 4623-4634
38. Puett, D., Friebele, E., and Hammonds, R.G., Jr. (1973) A comparison of the conformation; stabilities of homologous hemoproteins. Myoglobin from several species, human hemoglobin and subunits. *J. Mol. Biol.* **328**, 261-277
39. McLendon, G. (1977) A correlation between myoglobin thermodynamic stabilities and species metabolic rates. *Biochim. Biophys. Res. Commun.* **77**, 959-966
40. Stezkowski, F., Cassoly, R., and Banerjee, R. (1979) Binding of alkylisocyanides with soybean leghemoglobin. Comparison with sperm whale myoglobin. *J. Biol. Chem.* **254**, 1418-1426
41. Lecomte, J.T.J. and La Mar, G.N. (1985) ^{1}H NMR study of labile proton exchange in the heme cavity as a probe for the potential ligand entry channel in myoglobin. *Biochemistry* **24**, 7338-7395